

ARTICLE

Conceptional design of a He beam accelerator system for ^{211}At productionDaisuke Nagae^{a,*}, Aki Murata^a, Shota Ikeda^{a,b}, Shosuke Kikuchi^c, Ryoichi Yoshimura^c, Yoichi Ma^d,
Daigo Narita^d and Noriyosu Hayashizaki^a

^a Laboratory for Zero-Carbon Energy, Institute of Innovative Research, Tokyo Institute of Technology 2-12-1, Ookayama, Meguro-ku, Tokyo 152-8550 Japan; ^b Neutron Beam Technology Team, RIKEN Center for Advanced Photonics, RIKEN, 2-1, Hirosawa, Wako, Saitama, 351-0198 Japan; ^c Department of Radiation Therapeutics and Oncology, Division of Maxillofacial and Neck Reconstruction, Graduate School of Medical and Dental Sciences, Tokyo Medical and Dental University, 1-5-45, Yushima, Bunkyo-ku, Tokyo 113-8510 Japan; ^d School of Environment and Society, Tokyo Institute of Technology 2-12-1, Ookayama, Meguro-ku, Tokyo 152-8550 Japan

In the medical field, radiopharmaceuticals, which are medicinal drugs containing radioisotopes, are now widely recognised. These radiopharmaceuticals are administered and selectively concentrated in diseased areas such as cancer, and the alpha or beta rays from the radioisotopes are used to kill the cells. ^{211}At is one of the most promising radioisotopes for alpha radiotherapy due to its suitable half-life of $T_{1/2} = 7.214$ h and a substantive alpha-particle-emission probability of 100%. ^{211}At can be produced by the reaction, $^{209}\text{Bi}(\alpha, 2n)^{211}\text{At}$, using a He beam at an energy of approximately 28 MeV on the ^{209}Bi target. Conventional Cyclotrons are most commonly used for the production of ^{211}At . Due to an intrinsic limitation in a cyclotron, milliampere class ion beams cannot be accelerated and delivered, leading to the limited production yield of the ^{211}At . In addition, worldwide production of the ^{211}At is very limited and there are not enough facilities to meet demand. In order to produce large amount of ^{211}At , we are proposing a He beam accelerator system consists of an Electron Cyclotron Resonance (ECR) ion source with a high-current He beam, a Radio Frequency Quadrupole linear accelerator (RFQ) with a tuner less robust structure, and a Drift Tube linear accelerator (DTL) with the combined zero degree structure. This system aims to accelerate the alpha beam by up to 10 mA at continues wave mode on the production target.

Keywords: ^{211}At ; He beam accelerator; ECR ion source; RFQ; DTL

1. Introduction

Radionuclide therapy of alpha particle (targeted α -therapy: TAT) has been becoming popular. Since high linear energy transfer (LET) of α -particles undertakes severe damage to tumor cells, and short path length of them contributes to minimizing radiation damage to surrounding normal tissue, TAT appears to be suitable for disseminated disease, small neoplasms, micrometastases, and elimination of single tumor cells [1]. TAT with ^{223}Ra has been proven to improve the overall survival of patients with castration-resistant prostate cancer (CRPC) and bone metastases in clinical practice [2], and TAT is also being shown to be useful for the treatment of thyroid cancer, malignant glioma, pancreatic cancer, malignant myeloma, breast cancer, colon cancer, ovarian cancer, prostate cancer, and neuroendocrine tumor in vitro, vivo, and clinical trial [1-5].

There is a growing need for RI preparations that emit α -particle. As ^{223}Ra has a natural predilection for

osteoblastic bone turnover, ^{223}Ra does not need to be labelled to ensure targeting and has not been used in other TATs. Although ^{225}Ac has attracted attention for its labeling utility, and ^{225}Ac -PSMA is significantly effective even in refractory cases of ^{177}Lu -PSMA therapy for metastatic CRPC, its supply remains limited worldwide because its production requires nuclear fuel materials or rare radioisotopes. ^{211}At , on the other hand, can be produced by cyclotron and labeled to small molecules and peptides [6], and some labeled ^{211}At have been shown to be useful for the treatment in mice [7, 8].

An important property of ^{211}At is a substantive alpha-particle emission probability of 100%. **Figure 1** shows a decay scheme of ^{211}At . ^{211}At decays to ^{207}Bi ($T_{1/2} = 31.55(5)$ y) emitting a 5.87-MeV α particle with a decay probability of 41.8%. ^{207}Bi decays to ^{207}Pb by electron capture with a decay probability of 100%. ^{211}At also decays to ^{211}Po ($T_{1/2} = 516(3)$ ms) by electron capture with a decay probability of 58.2%, and then ^{211}Po decays to ^{207}Pb emitting a 7.45 MeV α particle with a decay probability of 100%. Most commonly, ^{211}At can be produced by the reaction, $^{209}\text{Bi}(\alpha, 2n)^{211}\text{At}$, using a He

*Corresponding author. E-mail: nagae.d.aa@m.titech.ac.jp

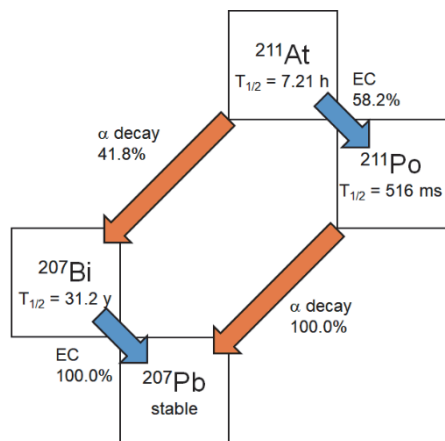
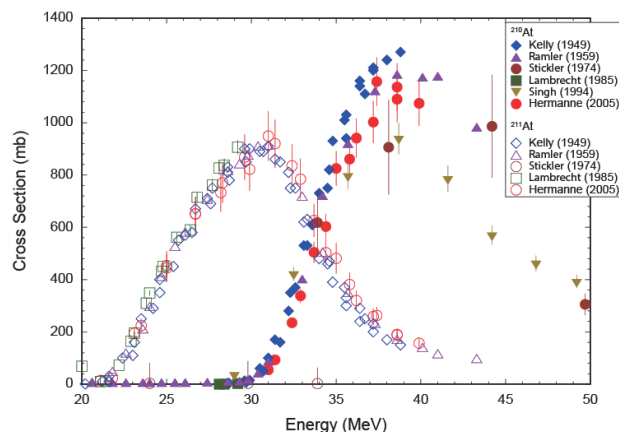
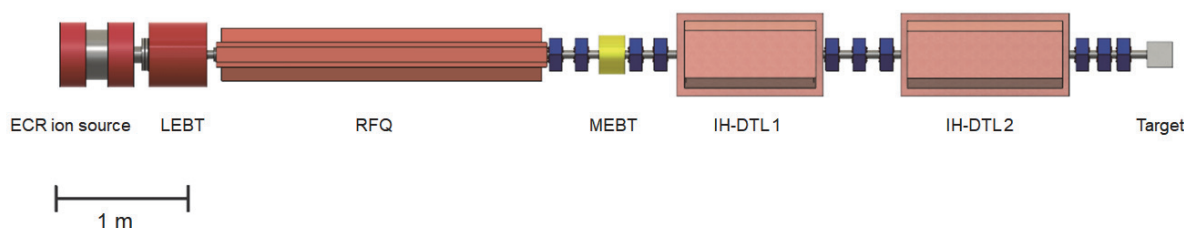
Figure 1. Decay scheme of ^{211}At .Figure 2. Production cross sections of ^{211}At and ^{210}At by $^{209}\text{Bi}(\alpha, 2n)^{211}\text{At}$ and $^{209}\text{Bi}(\alpha, 3n)^{210}\text{At}$ reactions. Data are taken from refs [9-14].

Figure 3. Structure design of the He beam accelerator system. A low energy beam transport line (LEBT) consists of two solenoid magnets. A medium energy beam transport line (MEBT) consists of two doublet quadrupole magnets and a rebuncher indicated in blue and yellow, respectively.

beam at an energy above 20 MeV on the ^{209}Bi target. The cross sections are illustrated in **Figure 2** with the reaction $^{209}\text{Bi}(\alpha, 3n)^{210}\text{At}$. The energy of the He beam is maintained below 29 MeV to avoid harmful ^{210}At ($T_{1/2} = 8.1(4)$ h) production that decays to long-lived ^{210}Po ($T_{1/2} = 138.376(2)$ d). The produced ^{211}At in the irradiated ^{209}Bi target is separated and purified by chemical processes. Since ^{211}At has a short half-life of 7.2 hours, it is important to have a high current beam intensity to shorten the beam irradiation time. This feature enables us to efficiently separate and prepare the RI formulations. Currently, the amount of ^{211}At required per dose is estimated to be about 50 MBq/kg [8]. Assuming a population of thyroid cancer patients of 10,000 per year in Japan [15], 4 times doses per year per person, and a body weight of 60 kg, 30 GBq of ^{211}At per day is required for 100 patients. Taking account of the time required for chemical separation, preparation into RI formulations, and transport from the production site to the hospital, it is estimated that about 10 times the required amount, 300 GBq of ^{211}At per day, would need to be produced.

The production of ^{211}At is mainly provided by conventional cyclotron facilities. In principle, the beam orbits of the n turn and that of $n+1$ turn in the cyclotron approach each other as the energy increases. In a high-current beam, the beam diameter increases due to the

space-charge effect, and beam loss is likely to occur at the beam extraction point. Therefore, the amount of beam current that can be accelerated by a cyclotron is typically limited to approximately several μA to 100 μA , which leads to the production yield of ^{211}At being restricted to approximately several GBq/h [16]. Considering that the half-life of ^{211}At is short compared to the time required to produce, purification, and transportation, it is desirable to have a production facility near the consumption area.

We are proposing a dedicated He beam accelerator system to produce several hundred GBq of ^{211}At . It is necessary to be able to precisely adjust the He-beam energy to maximize the production yield of ^{211}At with the minimized production yield of ^{210}At . In addition, this system is intended for installation within the university and must be of decent size. Therefore, a compact linear accelerator is employed in this system. This paper describes the physics design of the accelerator part of our production facility.

2. Description of the He beam accelerator system

A schematic view of the proposed He beam accelerator system is shown in **Figure 3**. The He beam accelerator system mainly consists of the Electron Cyclotron Resonance (ECR) ion source, the Radio Frequency Quadrupole linear

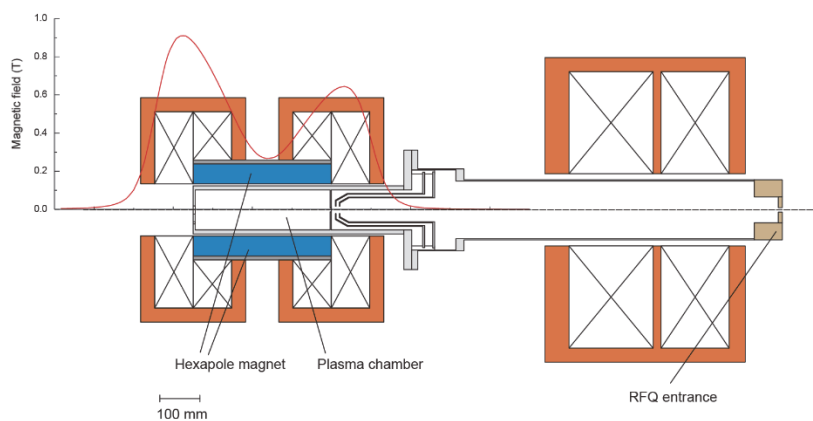


Figure 4. Design of ECR ion source and LEPT.

accelerator (RFQ), and two Drift Tube linear accelerators (DTL). This accelerator system is designed to accelerate the He beam up to 29 MeV with a beam intensity of 10 mA in continuous-wave (CW) mode. A beam energy of the He beam on the target can be adjusted with a gas degrader installed at the target area. Assuming the thickness of the ^{209}Bi target as 0.08 g/cm^2 , the He beam intensity 10 mA, the average cross section 400 mb, and the 2-hour purification time, the yield of ^{211}At is estimated to be 800 GBq/h using a simple calculation.

2.1. ECR ion source

The ECR ion source was designed to produce intense He beams with a charge state of $2+$. To meet the output beam current specification, the beam current demanded from the ion source was 15 mA with an estimated beam transmission efficiency of about 70% through the entire system. To provide a fully stripped He beam, 10 GHz of microwave frequency was selected for plasma heating. National Institute of Radiological Sciences (NIRS) reported that 2 mA of He^{2+} beam was successfully produced by an ECR ion source with a 10 GHz microwave at 230 W [17]. **Figure 4** shows a schematic drawing of our ECR ion source and low energy beam transport (LEBT). Because the beam intensity is proportional to a plasma volume, we designed a large plasma chamber. The inner diameter and length of the plasma chamber were 100 mm and 345 mm, respectively. The volume of the plasma chamber of the newly developed ECR ion source was approximately 4.6 times larger than the volume of the plasma chamber of the ECR ion source developed at NIRS. In addition, the beam intensity is also proportional to the microwave power [18, 19]. For the newly developed ECR ion source, 1-kW microwave power, which is about 4 times larger than the power used in NIRS, will be used for plasma heating. We plan to use three electrodes for the beam extraction system, which are platform (plasma chamber), intermediate, and electron repeller. The intermediate electrode will be used to adjust the extraction condition to minimise the beam emittance. A magnetic field distribution for a plasma confinement is generated by the solenoid coils and the hexapole magnet with the Halbach structure.

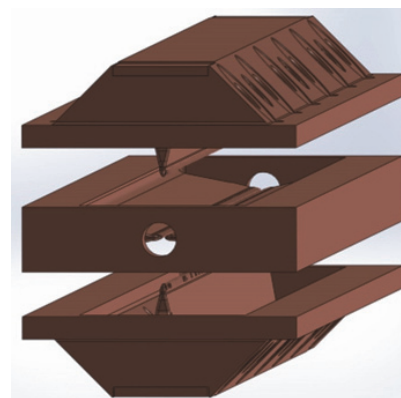


Figure 5. RFQ design. The RFQ consist of an upper minor vane, a major vane, and a lower minor vane.

2.2. RFQ

Figure 5 shows a schematic view of the RFQ. The structure of the RFQ is based on the three-layer configuration developed by Tokyo Institute of Technology and TIME co., Ltd. [20, 21]. Each of the three component parts is machined accurately from a single forged oxygen free copper block. The cooling channels are cut from the exterior of the cavity to maximize a flow rate of the cooling water. The three parts are precisely assembled by screws. The structure enables us to avoid unpredictable deformation caused by brazing. The RIKEN Accelerator-driven compact neutron source (RANS)-II (resonance frequency 200 MHz, duty 3.3%) has the same structure but was made of iron with copper plated interior. [22]. Considering power consumption, the electrode length was set at 3 m. In this design, the He^{2+} beam is accelerated from $E_{\text{total}} = 60 \text{ keV}$ to 4 MeV. To have a stable operation, Kilpatrick factor is selected at 1.8 which is not an aggressive value. The height of the vane and cavity diameter are 150 mm and 336 mm respectively. The resonance frequency is decided to have a relatively low value, which is 200 MHz, to have a good cooling efficiency. To avoid possible discharges, all stub tuners are eliminated which are generally used to control the electric field distribution. The stub tuners could lead to a local concentration of the surface current, and the RF contacts could cause serious damage on the RFQ when it operates at CW mode.

2.3. DTL

The He beam is accelerated from 4 MeV to 29 MeV by the DTL. An Inter-digital H-mode drift tube linear accelerator (IH-DTL) is used because of the high-power efficiency for a low velocity region. Since the beam intensity reaches about 10 mA, a beam focusing system is required in the DTL section to control the beam divergence caused by the space charge effect. To achieve beam focusing with IH-DTL, we typically have two choices, Alternative Phase Focusing (APF) scheme [23] and combined zero degree structure (KONUS) scheme [24]. In the APF scheme, by selecting positive and negative

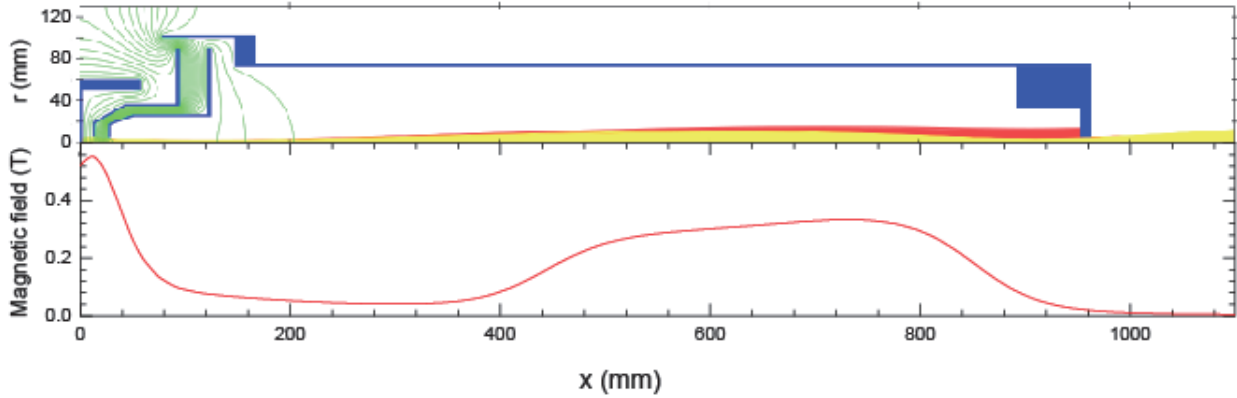


Figure 6. Simulation result of the transportation for He beam. The red and yellow line indicate He⁺ and He²⁺ beam trajectories, respectively.

RF phases of the gap voltages in the DTL, transverse and longitudinal beam focusing can be obtained simultaneously. However, there are few examples of its application to high current beams. In the KONUS scheme, the beam is accelerated near zero synchronous phase, which results in a higher shunt impedance compared to the APF scheme. However, an additional transverse focusing control knob is necessary.

Considering the availability of RF power sources on the market, we decided to split the DTL section into two RF cavities. Then each cavity can be driven by a single solid-state amplifier. In between the cavities, a triplet focusing magnet can be installed. We adopt the KONAS structure for the DTL.

As shown in Figure 3, the DTL section consists of the MEBT (the two doublet-quadrupole magnets and the rebuncher), IH-DTL1, the triplet-quadrupole magnet, and IH-DTL 2. By placing the quadrupole magnets outside of the cavities, a better heat load design can be easily achieved. The rebuncher at the MEBT is to match the longitudinal beam emittance with the IH-DTL acceptance. To synchronize the beam from the RFQ, the operating frequency of the DTL accelerator is also set at 200 MHz. The maximum electric field is $E = 23.6$ MV/m which is corresponded the Kilpatrick factor 1.6.

3. Simulations

3.1. ECR ion source

A magnetic configuration of the ECR ion source was designed by using an electromagnetic simulation code CST STUDIO SUITE [25]. The field strengths at upstream solenoid, downstream solenoid, and minimum B were $B_{\text{up}} = 0.91$ T, $B_{\text{down}} = 0.65$ T, and $B_{\text{min}} = 0.27$ T, respectively. The radial magnetic fields created by the hexapole magnet at the plasma chamber wall was 0.71 T. The obtained magnetic field strength was sufficient for confinement of the plasma generating the 10-GHz microwave.

A beam transport from the ECR ion source to the RFQ was simulated by using IBSimu code [26]. In this simulation, the initial beam intensities were set as 24.0 mA and 16.0 mA for He⁺ and He²⁺, respectively, to reproduce the

experimental beam-intensity ratio founded at the NIRS [17]. The initial position distribution of the He beams was set same as the extraction hole of the plasma chamber. The initial energy was set at $E = 10$ eV, and the initial angle was set to be perpendicular to the extraction hole of the plasma chamber. Thus, the calculated transmission efficiency was considered to be ideal values. The diameters of the extraction hole of the plasma chamber, an intermediate electrode, and the electron repeller electrode were chosen to be 10 mm, 12 mm, and 10 mm, respectively. The electrode potential and the magnetic field of the LEBT were adjusted to be only sufficiently small relative to the design normalised RMS emittance of the RFQ which is $\epsilon = 0.125 \pi$ mm mrad. The electrode potentials were set to be 30 kV, 22.5 kV, and -5 kV for the plasma chamber, the intermediate electrode, and the electron repeller electrode, respectively. **Figure 6** shows the beam trajectories at the LEBT region. The transmission efficiencies of He⁺ and He²⁺ beam from ion source to LEBT end (RFQ entrance) were calculated to be 35% and 99%, respectively, resulting the beam intensity 8.3 mA and 15.9 mA. The beam emittances at the RFQ entrance were calculated to be $\epsilon = 0.082 \pi$ mm mrad for He⁺ and $\epsilon = 0.067 \pi$ mm mrad for He²⁺. Although these results about He²⁺ beam satisfies the requirements of the beam transportation, large amount of the He⁺ beam was injected into the RFQ or stopped at the RFQ vane. To avoid He⁺ injection into the RFQ, a collimator will be introduced in the LEBT. In this simulation, the initial conditions of the beam were set to ideal values, however, depending on the plasma conditions, the initial conditions may take on various values. Further beam transport simulation taking account a plasma condition is ongoing using the same IBSimu code [26].

3.2. RFQ

In designing the feasibility of the RFQ, the beam dynamics was first verified using a technically established software suite called PARMTEQ [27]. Although the code uses a very simplified space-charge effect and cannot include image charges, many groups use it as a benchmark of the RFQ simulations. The transmission efficiency was

Table 1. RFQ design parameter.

Particle	He ²⁺
Injection energy	60 keV
Extraction energy	4 MeV
Phase	-90~-20 degree
Duty	100%
Electric field at vane	26.5 MV/m
Inter vane voltage	57 kV
Inject / extract beam current	12.0 / 11.4 mA
Transmission efficiency	94.9%
Twiss parameter (hor)	$\alpha = 1.4402$ $\beta = 103.285$ mm/rad
Twiss parameter (ver)	$\alpha = -1.68$ $\beta = 116$ mm/rad
Normalized RMS emittance	0.137 π mm mrad (hor.) 0.133 π mm mrad (ver.)
Length of vane	2840 mm

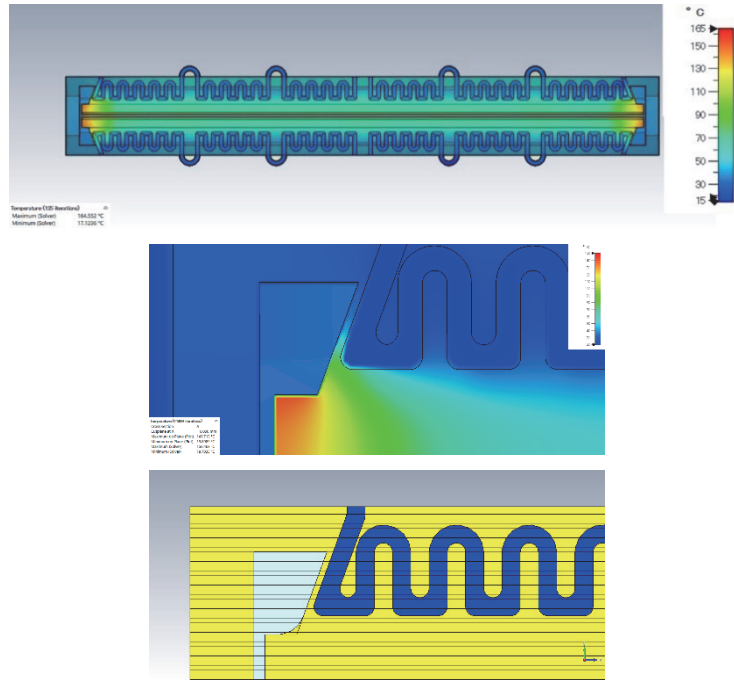


Figure 7. (Top) Surface temperature distribution. (Middle) Zoom up around the vane tip. (Bottom) Idea of the shape modification.

maximised by scanning the Twiss parameters of the injected beam. The assumed normalised RMS emittance of the injecting beam is $\epsilon = 0.125 \pi$ mm mrad for both horizontal and vertical planes. A transmission efficiency of 94.9% was achieved in the Twiss parameters presented in **Table.1**. The injection beam was 12.0 mA while the output beam was 11.4 mA. The normalised RMS emittances at the RFQ exit were calculated to be $\epsilon_{hor} = 0.137 \pi$ mm mrad and $\epsilon_{ver} = 0.133 \pi$ mm mrad for the horizontal and vertical planes, respectively. The predicted beam performance of the RFQ satisfies the requirements of the entire accelerator system. More detailed optics simulation is in progress using some latest simulation codes to further improve the performance.

The most challenging problem in delivering the CW beam is the heat removal of the RFQ cavity. We have learnt that the temperature rise at the end of the vane tip is the most critical in a four-vane-type RFQ cavity. A thermal analysis of the RFQ was performed using a conjugate heat transfer solver of the CST STUDIO SUITE [25] in conjunction with the simulated electromagnetic fields. **Figure 7** (Top) shows a thermal-analysis result assuming an ambient temperature at 20°C, an input water temperature at 20°C with a flow rate of 50 liter/min, and a wall loss of 200 kW. The surface temperature distribution at the vane surfaces was uniform at approximately 60°C, except at the end which is approximately 165°C (see **Figure 7** (Middle)). The outer wall of the RFQ reached 40°C. A local deformation of the vane was estimated to be 0.2 mm at maximum. A frequency shift due to the deformation was 0.127 MHz which is acceptable value for the accelerator operation. A simple polygon shape of the vane tip was applied in this simulation. In a realistic

geometry with vertices connected by curves, the heat diffusion could be improved and mitigate the highest temperature at the vane end as shown in **Fig. 7** (Bottom). Details of the thermal analysis are described in Ref. [28].

3.3. DTLs

The beam trajectory calculations for IH-DTL 1 and 2 including the space charge effect were performed using General Particle Tracer [29]. The beam transport sections from the RFQ to the IH-DTL1 and to the IH-DTL2 are occupied by the MEBT and the triplet quadrupole magnets to manipulate the matching condition of the following each linear accelerator. The design parameters of the IH-DTLs are summarised in **Table. 2**. The electric potentials of IH-DTLs calculated by CST [25] were imported to the General Particle Tracer. **Figures 8** (a) and (b) are the beam trajectories in the IH-DTL 1 and 2, respectively. In IH-DTL 2, the acceleration phase of the injection beam and the electric field intensity between the gaps were optimised to squeeze the energy spread of the output beam. The accelerated energy was calculated to be 28.75 MeV with an energy spread ± 0.25 MeV as shown in **Figure 9**. The transmission efficiencies of IH-DTL 1 and 2 were achieved 92.3% and 100%, respectively. The predicted beam intensity was 12 mA, which was 100 times higher than that of conventional cyclotrons. Large amount of ²¹¹At about several hundred GBq/h will be produced by using the proposed He beam accelerator system.

4. Conclusion

We have designed the He beam accelerator system for ²¹¹At production based on state-of-the-art RF linear

Table 2. DTL design parameter.

	IH-DTL 1	IH-DTL 2
Resonant frequency [MHz]	200	←
Duty [%]	100	←
Structure	IH	←
Total length [mm]	1012	1300
Gap length [mm]	21.2	←
Cell number	18	Rebunch: 3 Accelerator: 13
Drift tube aperture [mm]	16	←
Gap voltage [kV]	500	←
Electric field strength [MV/m]	23.6	←
Synchronous phase [deg]	0	Rebunching section: -35 Accelerator section: 0
Input beam energy [MeV]	4.0	17
Output beam energy [MeV]	17	28.75
Beam current [mA]	12	←

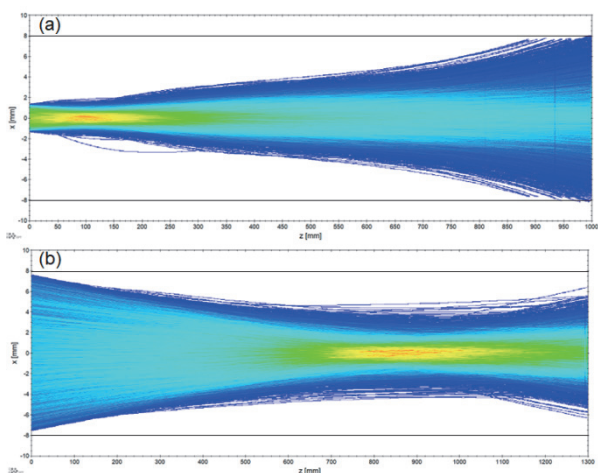


Figure 8. Beam envelopes in IH-DTL1 (a) and IH-DTL2 (b). The solid lines at ± 8 mm in x axis indicate the diameter of the drift tube.

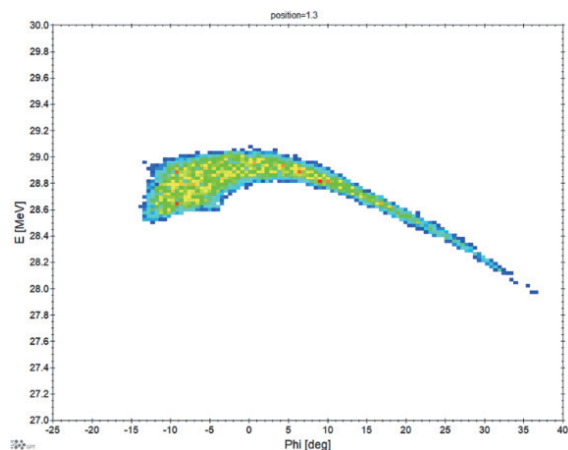


Figure 9. Beam energy.

accelerator technology. The system consists of the 10 GHz ECR ion source, the less structured tuner RFQ, and IH-DTLs with the KONUS scheme. Simulations of beam extraction, acceleration by the RFQ, and acceleration by the IH-DTL were performed. The calculated beam energy was reached at 28.75 MeV with an energy spread ± 0.25 MeV with a beam intensity of 12 mA. This intensity was sufficient in production of ^{211}At at the several hundred GBq. The feasibility simulation study has been completed, and more detailed simulation and experimental studies are underway.

References

- [1] J.L. Hatcher-Lamarre, V.A. Sanders, M. Rahman, C.S. Cutler and L.C. Francesconi, Alpha emitting nuclides for targeted therapy, *Nucl Med Biol.* 92 (2021), pp. 228-240.
- [2] C. Parker, S. Nilsson, D. Heinrich, S.I. Helle, J.M. O'Sullivan, S.D. Fosså, A. Chodacki, P. Wiechno, J. Logue, M. Seke, A. Widmark, D.C. Johannessen, P. Hoskin, D. Bottomley, N.D. James, A. Solberg, I. Syndikus, J. Kliment, S. Wedel, S. Boehmer, M. Dall'Oglio, L. Franzén, R. Coleman, N.J. Vogelzang, C.G. O'Bryan-Tear, K. Staudacher, J. Garcia-Vargas, M. Shan, Ø.S. Bruland and O. Sartor for the ALSYMPCA Investigators, Alpha emitter radium-223 and survival in metastatic prostate cancer, *N Engl J Med* 369 (2013), pp. 213-223.
- [3] T. Watabe, K. Kaneda-Nakashima, Y. Liu, Y. Shirakami, K. Ooe, A. Toyoshima, E. Shimosegawa, M. Fukuda, A. Shinohara and J. Hatazawa, Enhancement of ^{211}At uptake via the sodium iodide symporter by the addition of ascorbic acid in targeted α -therapy of thyroid cancer, *J Nucl Med* 60 (2019), 1301-1307.
- [4] K. Kaneda-Nakashima, Z. Zhang, Y. Manabe, A. Shimoyama, K. Kabayama, T. Watabe, Y. Kanai, K. Ooe, A. Toyoshima, Y. Shirakami, T. Yoshimura, M. Fukuda, J. Hatazawa, T. Nakano, K. Fukase and A. Shinohara, α -emitting cancer therapy using ^{211}At -AAMT targeting LAT1, *Cancer Sci* 112 (2021), pp. 1132-1140.
- [5] S. Navalkissoor and A. Grossman, Target alpha particle therapy for neuroendocrine tumors: the next generation of peptide receptor radionuclide therapy, *Neuroendocrinology* 108 (2019), 256-564.
- [6] M.R. Zalutsky and M. Pruszynski, Astatine-211: production and availability, *Curr Radiopharm* 4 (2011), 177-185.
- [7] H. Sudo, A.B. Tsuji, A. Sugyo, K. Nagatsu, K. Minegishi, N.S. Ishioka, H. Ito, K. Yoshinaga and T. Higashi, Preclinical Evaluation of the Acute Radiotoxicity of the α -Emitting Molecular-Targeted Therapeutic Agent ^{211}At -MABG for the Treatment of Malignant Pheochromocytoma in Normal Mice, *Translational Oncology* 12 (2019), 879-888.
- [8] T. Watabe, Y. Liu, K. Kaneda-Nakashima, T. Sato, Y. Shirakami, K. Ooe, A. Toyoshima, E. Shimosegawa, Y. Wang, H. Haba, T. Nakano, A. Shinohara and J. Hatazawa, Comparison of the Therapeutic Effects of

- [²¹¹At]^{NaAt} and [¹³¹I]^{NaI} in an NIS-Expressing Thyroid Cancer Mouse Model, *International Journal of Molecular Sciences* 23 (2022), p.9434.
- [9] E.L. Kelly and E. Segre, Some Excitation Functions of Bismuth, *Physical. Review* 75 (1949), pp. 999-1005.
- [10] W.J. Ramler, J. Wing, D.J. Henderson and J.R. Huizenga, Excitation Functions of Bismuth and Lead, *Physical. Review* 114 (1959), pp.154-162.
- [11] J.D. Stickler and K.J. Hofstetter, Comparison of He-, He-, and C-induced nuclear reactions in heavy-mass targets at medium excitation energies. I. Experimental cross sections, *Physical. Review C* 9 (1974), pp.1064-1071.
- [12] R.M. Lambrecht and S. Mirzadeh, Cyclotron Isotopes and Radiopharmaceuticals-XXXV Astatine-211, *International Journal of Applied Radiation and Isotopes* 36 (1985), pp.443-450.
- [13] N.L. Singh, S. Mukherjee and D.R.S. Somayajulu, Non-Equilibrium Analysis of (α , xn) Reactions on Heavy Nuclei, *Nuovo Cimento A* 107 (1994), pp.1635-1645.
- [14] A. Hermanne, F. Tarkanyi, S. Takacs, Z. Szucs, Y.N. Shubin and A.I. Dityuk, Experimental study of the cross-sections of α -particle induced reactions on ²⁰⁹Bi, *Applied Radiation and Isotopes* 63 (2005), pp. 1-9.
- [15] Cancer Statistics. Cancer Information Service, National Cancer Center, Japan (National Cancer Registry, Ministry of Health, Labour and Welfare), https://ganjoho.jp/reg_stat/statistics/data/dl/en.html
- [16] Y. Feng and M.R. Zalutsky, Production, purification and availability of ²¹¹At: Near term steps towards global access, *Nuclear Medicine and Biology* 100-101 (2021), pp. 12-23.
- [17] M. Muramatsu, S. Hojo, Y. Iwata, K. Katagiri, Y. Sakamoto, N. Takahashi, N. Sasaki, K. Fukushima, K. Takahashi, T. Suzuki, T. Sasano. T. Uchida, Y. Yoshida, S. Hagino, T. Nishiokada, Y. Kato and A. Kitagawa, Development of a compact ECR ion source for various ion production, *Review of Scientific Instruments* 87 (2016), 02C110.
- [18] Y. Torii, M. Shimada, I. Watanabe, J. Hipple, C. Hayden and G. Dionne, A high-current density and long lifetime ECR source for oxygen implanters, *Review of Scientific Instruments* 61 (1990), pp. 253-255.
- [19] L.T. Sun, H.W. Zhao, Z.M. Zhang, H. Wang, B.H. Ma, X.Z. Zhang, X.X. Li, Y.C. Feng, J.Y. Li, X.H. Guo, Y. Shang and H.Y. Zhao, 36-segmented high magnetic field hexapole magnets for electron cyclotron resonance ion source, *Review of Scientific Instruments* 78 (2007), 053302.
- [20] Patent JP5317062B2, US8928216B2
- [21] M. Masuoka and H. Yamauchi, DEVELOPMENT OF COMMERCIAL RFQ TOWARD CW APPLICATIONS, LINAC 2022 MOPOR112.
- [22] T. Kobayashi, S. Ikeda, Y. Otake, Y. Ikeda and N. Hayashizaki, Completion of a new accelerator-driven compact neutron source prototype RANS-II for on-site use, *Nuclear Instruments and Methods in Physics Research A* 994 (2021), 165091.
- [23] H. Deitinghoff, P. Junior and H. Klein, Properties of heavy ion linacs with alternating phase focusing" Proceedings of the 1976 Proton Linear Accelerator Conference (LINAC'76) Chalk River, Canada (JACoW, Geneva, 013), (1976), p. 238.
- [24] U. Ratzinger, H. Hähnel, R. Tiede, J. Kaiser and A. Almomani, Combined zero degree structure beam dynamics and applications, *Physical Review Accelerators and Beams* 22 (2019), 114801.
- [25] <https://www.3ds.com/ja/products-services/simulia/products/cst-studio-suite/>
- [26] T. Kalvas, O. Tarvainen, T. Ropponen, O. Steczkiewicz, J. Ärje and H. Clark, IBSIMU: A three-dimensional simulation software for charged particle optics, *Review of Scientific Instrument* 81 (2010), 02B703 2010.
- [27] K.R. Crandall, PARMTEQ-A beam dynamics code for the RFQ linear accelerator, *Joanne Evans and Lester Hunt (eds) International Handbook on the Economics of Energy*, Cheltenham, Edward Elgar.
- [28] A. Murata (2023) in this proceeding.
- [29] <http://pulsar.nl/gpt>